MASTERARBEIT / MASTER THESIS

Titel der Masterarbeit / Title of the Master Thesis

"The atmospheric Ekman spiral for piecewise-uniform eddy viscosity"

verfasst von / submitted by

Eduard Stefanescu, BSc

angestrebter akademischer Grad / in partial fulfilment of the requirements for the degree of

Master of Science (MSc)

Wien, 2023 / Vienna, 2023

Studienkennzahl lt. Studienblatt / degree programme code as it appears on the student record sheet:	UA 066 821
Studienrichtung lt. Studienblatt / degree programme as it appears on the student record sheet:	Masterstudium Mathematik
Betreut von / Supervisor:	Univ.-Prof. Adrian Constantin, PhD

Abriss

Im Jahr 1905 untersuchte Ekman das Verhalten von Winddrift Meeresströmungen, um Nansens Vermutung eines Ablenkwinkels der Strömung an der Meeresoberfläche in arktischen Regionen zu erklären, siehe [10]. Er schrieb eine genaue Lösung der Geschwindigkeitskomponenten nieder, die von ihrer Höhe abhängen, sofern wir konstante eddy Viskosität annehmen. 2020 fanden D.G. Dritschel, N. Paldor und A. Constantin [9] eine explizite Lösung zu den tiefenabhängigen Geschwindigkeitskomponenten für variable eddy Viskosität und auch für den Ablenkwinkel, i.e. das Verhalten der Ekman Spirale unter der Meeresoberfläche. In dieser Arbeit leiten wir eine Lösung für die Geschwindigkeitskomponenten in der Atmosphäre her, untersuchen den Ablenkwinkel und stellen sein Verhalten graphisch dar. Nach einer knappen Motivation präsentieren wir unterschiedliche Schichten der Atmosphäre, wir führen die Navier-Stokes Gleichungen in rotierenden sphärischen Koordinaten ein und leiten die dimensionslosen Bewegungsgleichungen für gleichförmige Strömungen in der Ekman Schicht in nicht äquatorialen Gebieten auf der Nordhalbkugel her. Hier halten wir uns an [5] und [7]. Der dritte Abschnitt behandelt die exakte Lösung der Bewegungsgleichungen und die relevanten Anfangsbedingungen in der f-plane Approximation, indem wir ähnlich vorgehen wie [9]. Im vierten Abschnitt berechnen wir die Ekman Spirale für die gelösten Geschwindigkeitskomponenten. Der fünfte Abschnitt behandelt Interpretationen des Verhaltens des Ablenkwinkels an der Oberfläche und der Ekman Spirale im Allgemeinen, welche von Höhe, eddy Viskosität und dem "Sprung-Punkt" der stückweisen konstanten eddy Viskosität abhängen, durch explizite Berechnungen und Graphen. Eine zusammenfassende Schlussfolgerung ist im sechsten Abschnitt zu finden.

Abstract

In 1905 Ekman investigated the behaviour of wind-drift ocean currents, in the attempt to explain Nansen's observation of the surface current deflection to the right in arctic regions, see [10]. He wrote down an explicit solution for the velocity components dependent on height, assuming a constant eddy viscosity. In 2020, D.G. Dritschel, N. Paldor, and A. Constantin [9] found an explicit solution to the depth-dependent velocity components for variable eddy viscosity and for the deflection angle, i.e. the behaviour of the Ekman spiral under the sea surface. In this thesis we derive an explicit solution to the velocity components in the atmosphere, investigate the deflection angle and graph the behaviour. After a brief motivation, we present the various atmospheric layers, we introduce the Navier-Stokes equations in rotating spherical coordinates and derive the dimensionless equations of motion for steady flow in the Ekman layer of non-equatorial regions of the northern hemisphere. Here we heavily rely on [5] and [7]. The third section deals with the exact solution of the equations of motion and the relevant boundary conditions in the f-plane approximation, in a very similar manner as [9]. In the fourth section we calculate the Ekman spiral for the solved velocity components. The fifth section deals with interpretations of the behaviour of the deflection angle on the surface and the Ekman-spiral in general, which are dependent on height, eddy viscosity and the jump point of the piecewise-constant eddy viscosity, by explicit calculations and graphs. Some summarizing conclusions are provided in Section 6.

Contents

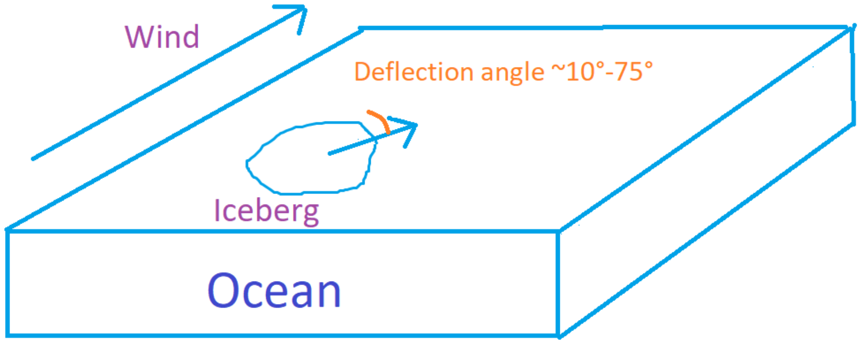

Figure 1: Nansen's observation: An Iceberg does not flow in the wind-direction. There is a deflection angle due to Coriolis forces.

1 Introduction

1.1 History

Before the famous paper "On the Influence of the Earth's Rotation on Ocean-Currents" by Ekman [10], Coriolis forces were known, but were neglected in calculations for currents. Nevertheless, drifts to the right were pointed out, see [2], but were explained not as an effect of Earth's rotation, rather as a result of other cooperating circumstances. During the arctic expeditions of Fridtjof Nansen during 1893-1896, - see [17], [12], [18], [22]- he observed that the drift of icebergs were at some angle to the right of the surface winds, see figure 1. He explained it as a consequence of earth's rotation and also concluded that the deviation angle must be larger in the water below. Based on Fridtjof Nansen's suggestion, Vagn Walfried Ekman investigated the problem mathematically and confirmed Nansen's observations. This same phenomenon can be observed for wind currents as well. In Ekman's paper [10], the eddy viscosity was taken to be constant, which makes solving equations, that we also derive in the first section, "quite simple" (We have to solve a non-homogeneous linear ordinary differential equation of second order, which we presuppose the reader to know, nevertheless it is explained in [29]). In this case Ekman evaluated the deviation angle of the surface winds and water drifts to be 45°. Subsequent studies have shown that a deflection angle of $10° - 75°$ can occur, see [26], [31].
One way to approach this problem is to take a look at atmospheric layers and vary the eddy viscosity.

1.2 Different wind layers and eddy viscosity

The following is based on [16],[20]. The atmosphere can be divided into essentially three layers. The laminar sub layer with a thickness of a few millimetres is the lowest one. But since all physical processes are dependent on molecular motion, it is not relevant for the transfer of wind energy. The Prandtl layer is around 10m, depending on the thermal stratification of the air. The upper layer is called the Ekman layer, where the airflow is driven by a balance of turbulent drag, Coriolis forces and pressure gradients. It ranges from the Prandl layer to $100 - 1000$m (depending on the location and local conditions) and covers 90% of the atmospheric boundary layer.
In the introduction of [4] there are different kinds of eddy viscosity with different behaviours listed: There are suggestions that the eddy viscosity can increase, decrease and even other different behaviours, see [1], [14], [28], [23], [11] and [19]. Furthermore numerical simulations were made in [15], [30] and [3].

1.3 Our approach

A more realistic eddy viscosity than constant, as in Ekman's paper [10], is piecewise constant eddy viscosity. Considering this, we will calculate an explicit solution to the velocity components and a solution to the Ekman spiral in the atmosphere depending on height over the surface, the values of the eddy viscosity and the height, where it changes. The eddy viscosity can be any step-function with a finite amount of steps. This means any kind of occurring eddy viscosity can be approximated by this method and consequently the velocity components as well as the Ekman spiral can also be approximated by this method. We will see in the "Interpretation"-section that there is indeed an influence on the deflection angle. It can change its value by this approach by differing the above mentioned dependent variables.

2 Derivation of the equations of motion

The following part is based on [5] and [7]. For a physical interpretation of Navier-Stokes and all associated equations, we refer to [7].

2.1 Spherical coordinates

Remark 2.1. *: Physical variables, the ones that have dimensions, are denoted with a "tilde". Dimensionless variables do not have "tildes".*

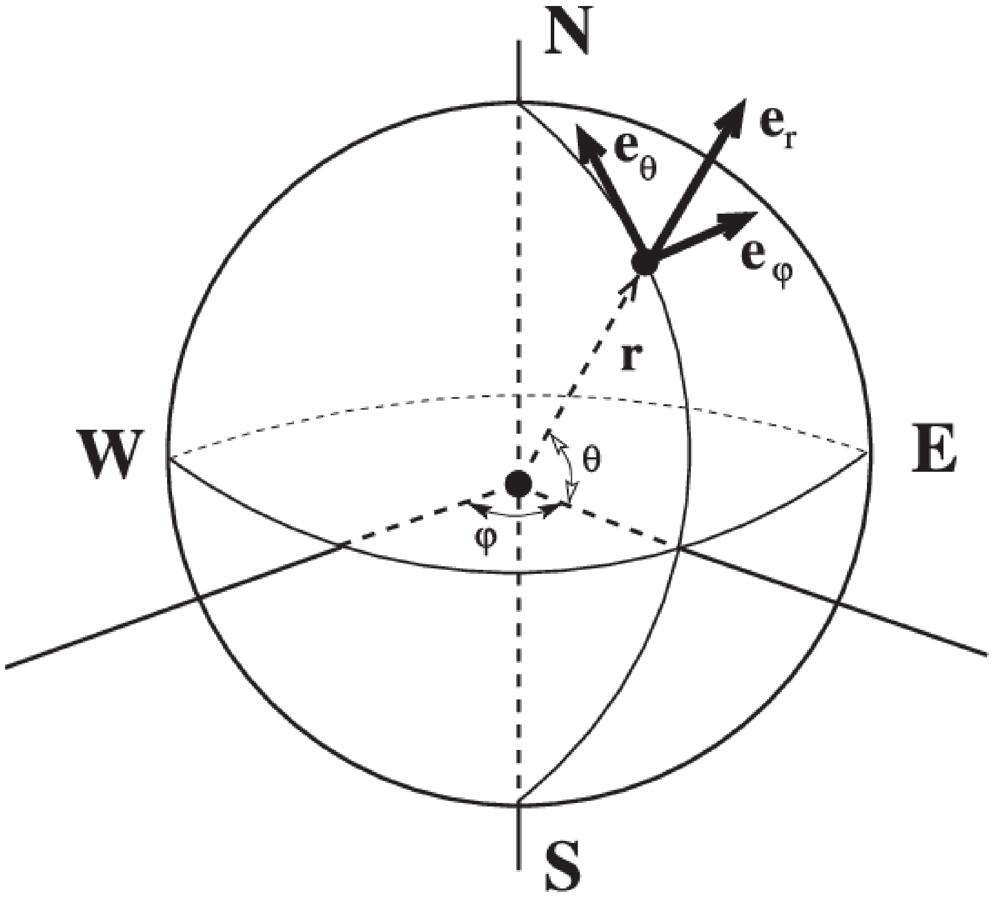

Figure 2: The spherical coordinate system with $\phi, \theta, \tilde{r}$, where $\phi \in [0, 2\pi)$ being the azimuthal angle, $\theta \in [-\frac{\pi}{2}, \frac{\pi}{2}]$ being the polar angle and $\tilde{r}$ being the radial distance. The unit vectors are e_ϕ, e_θ and e_r. This graphic is taken from [5].

We start by introducing right-handed spherical coordinates $\phi, \theta, \tilde{r}$, where $\phi \in [0, 2\pi)$ is the angle of longitude or also known as the azimuthal angle, $\theta \in [-\pi/2, \pi/2]$ is the angle of latitude or polar angle and $\tilde{r}$ is the radial distance, i.e. the distance from the center of the sphere. The unit vectors are denoted by e_ϕ, e_θ, e_r, where e_ϕ is pointing east, e_θ pointing north and e_r upwards, see Figure 2. The corresponding velocity components are $\tilde{u}, \tilde{v}, \tilde{w}$.

Remark 2.2. *: We avoid the north and the south pole, because e_ϕ and e_θ are not well defined there. This type of singularity is unavoidable, due to the "hairy ball theorem" from differential topology (see Milnor [21]).*

2.2 The Navier-Stokes equations in rotating spherical coordinates

2.2.1 Physical introduction

The Navier-Stokes equations are an application of Newtons second law, i.e. force=acceleration×mass. Before writing down the exact solutions we introduce all the needed variables: $\tilde{F}_\phi, \tilde{F}_\theta, \tilde{F}_r$ are the body forces, $\tilde{\rho}$ is the density, $\tilde{p}(\phi, \theta, \tilde{r}, t)$ is the pressure in the fluid and $\tilde{v}_1$ and $\tilde{v}_2$ are the vertical and the horizontal kinematic eddy viscosities.
In spherical coordinates Navier-Stokes Equations can be written like this:

$$\begin{aligned}\frac{\partial \tilde{u}}{\partial \tilde{t}} + \frac{\tilde{u}}{\tilde{r}\cos\theta}\frac{\partial \tilde{u}}{\partial \phi} + \frac{\tilde{v}}{\tilde{r}}\frac{\partial \tilde{u}}{\partial \theta} + \tilde{w}\frac{\partial \tilde{u}}{\partial \tilde{r}} + \frac{1}{\tilde{r}}\left(-\tilde{u}\tilde{v}\tan\theta + \tilde{u}\tilde{w}\right) \\ = -\frac{1}{\tilde{\rho}}\frac{1}{\tilde{r}\cos\theta}\frac{\partial \tilde{p}}{\partial \phi} + \tilde{F}_\phi + \tilde{\nu}_1\frac{\partial^2 \tilde{u}}{\partial \tilde{r}^2} + \frac{2\tilde{\nu}_1}{\tilde{r}}\frac{\partial \tilde{u}}{\partial \tilde{r}} \\ + \frac{\tilde{\nu}_2}{\tilde{r}^2}\left(\frac{1}{\cos^2\theta}\frac{\partial^2 \tilde{u}}{\partial \phi^2} - \tan\theta\frac{\partial \tilde{u}}{\partial \theta} + \frac{\partial^2 \tilde{u}}{\partial \theta^2}\right),\end{aligned} \tag{2.1}$$

$$\begin{aligned}\frac{\partial \tilde{v}}{\partial \tilde{t}} + \frac{\tilde{u}}{\tilde{r}\cos\theta}\frac{\partial \tilde{v}}{\partial \phi} + \frac{\tilde{v}}{\tilde{r}}\frac{\partial \tilde{v}}{\partial \theta} + \tilde{w}\frac{\partial \tilde{v}}{\partial \tilde{r}} + \frac{1}{\tilde{r}}\left(\tilde{u}^2\tan\theta + \tilde{v}\tilde{w}\right) \\ = -\frac{1}{\tilde{\rho}}\frac{1}{\tilde{r}}\frac{\partial \tilde{p}}{\partial \theta} + \tilde{F}_\theta + \tilde{\nu}_1\frac{\partial^2 \tilde{v}}{\partial \tilde{r}^2} + \frac{2\tilde{\nu}_1}{\tilde{r}}\frac{\partial \tilde{v}}{\partial \tilde{r}} \\ + \frac{\tilde{\nu}_2}{\tilde{r}^2}\left(\frac{1}{\cos^2\theta}\frac{\partial^2 \tilde{v}}{\partial \phi^2} - \tan\theta\frac{\partial \tilde{v}}{\partial \theta} + \frac{\partial^2 \tilde{v}}{\partial \theta^2}\right),\end{aligned} \tag{2.2}$$

$$\begin{aligned}\frac{\partial \tilde{w}}{\partial \tilde{t}} + \frac{\tilde{u}}{\tilde{r}\cos\theta}\frac{\partial \tilde{w}}{\partial \phi} + \frac{\tilde{v}}{\tilde{r}}\frac{\partial \tilde{w}}{\partial \theta} + \tilde{w}\frac{\partial \tilde{w}}{\partial \tilde{r}} + \frac{1}{\tilde{r}}(-\tilde{u}^2 - \tilde{v}^2) \\ = -\frac{1}{\tilde{\rho}}\frac{\partial \tilde{p}}{\partial \tilde{r}} + \tilde{F}_r + \tilde{\nu}_1\frac{\partial^2 \tilde{w}}{\partial \tilde{r}^2} + \frac{2\tilde{\nu}_1}{\tilde{r}}\frac{\partial \tilde{w}}{\partial \tilde{r}} \\ + \frac{\tilde{\nu}_2}{\tilde{r}^2}\left(\frac{1}{\cos^2\theta}\frac{\partial^2 \tilde{w}}{\partial \phi^2} - \tan\theta\frac{\partial \tilde{w}}{\partial \theta} + \frac{\partial^2 \tilde{w}}{\partial \theta^2}\right).\end{aligned} \tag{2.3}$$

The Equation of mass conservation is the following:

$$\frac{1}{\tilde{r}\cos\theta}\frac{\partial \tilde{u}}{\partial \phi} + \frac{1}{\tilde{r}\cos\theta}\frac{\partial}{\partial \theta}(\tilde{v}\cos\theta) + \frac{1}{\tilde{r}^2}\frac{\partial}{\partial \tilde{r}}(\tilde{r}^2\tilde{w}) = 0. \tag{2.4}$$

We now fix e_ϕ, e_θ, e_r as a point on the sphere that is rotating about its polar axis. For this, we need a Coriolis and a centripetal acceleration term, which are $2\tilde{\mathbf{\Omega}} \times \tilde{\mathbf{u}}$ and $\tilde{\mathbf{\Omega}} \times (\tilde{\mathbf{\Omega}} \times \tilde{\mathbf{r}})$, where $\tilde{\mathbf{\Omega}} = \tilde{\Omega}(e_\theta\cos\theta + e_r\sin\theta)$, $\tilde{\mathbf{u}} = \tilde{u}e_\phi + \tilde{v}e_\theta + \tilde{w}e_r$ and $\tilde{\mathbf{r}} = \tilde{r}e_r$ respectively. We must add this to the left side of (2.1), (2.2) and (2.3). We can imagine these equations as a 3−vector, hence adding the above makes sense. The variable $\tilde{\Omega} \approx 7.29 \times 10^{-5}$rad/s is the constant rate of rotation of the earth. The sum of the two new terms is:

$$\begin{aligned} &2\tilde{\Omega}(-\tilde{v}\sin\theta + \tilde{w}\cos\theta, \tilde{u}\cos\theta, \tilde{u}\sin\theta, -\tilde{u}\cos\theta) \\ &\qquad +\tilde{r}\tilde{\Omega}^2(0, \sin\theta\cos\theta, -\cos^2\theta). \end{aligned} \tag{2.5}$$

The body-forces are chosen in the following way: $\tilde{F}_\phi = 0$, $\tilde{F}_\theta = 0$ and $\tilde{F}_r = -\tilde{g}$, where $\tilde{g} \approx 9.81\text{m/s}$. We choose $\tilde{g}$ to be constant, which is justified by the depths of the ocean and the vertical atmospheric range of the earth in which we derive solutions. Because we are interested in heights above (and under) the Earth's surface, it makes sense to define $\tilde{r} = \tilde{R} + \tilde{z}$, with $\tilde{R} \approx 6.378 \times 10^6\text{m}$, being the mean[1] radius of the earth. At the free surface[2], where $\tilde{r} = \tilde{R} + \tilde{h}(\phi, \theta, \tilde{t})$, we introduce surface pressure $\tilde{P}_s$ and the kinematic boundary condition:

$$\tilde{p} = \tilde{P}_s(\phi, \theta, \tilde{t}) \quad \text{on} \quad \tilde{r}(\phi, \theta, \tilde{t}) = \tilde{R} + \tilde{h}(\phi, \theta, \tilde{t}), \tag{2.6}$$

$$\tilde{w} = \frac{\partial \tilde{h}}{\partial \tilde{t}} + \frac{\tilde{u}}{\tilde{r}\cos\theta}\frac{\partial \tilde{h}}{\partial \phi} + \frac{\tilde{v}}{\tilde{r}}\frac{\partial \tilde{h}}{\partial \theta} \quad \text{on} \quad \tilde{r}(\phi, \theta, \tilde{t}) = \tilde{R} + \tilde{h}(\phi, \theta, \tilde{t}). \tag{2.7}$$

Moreover, the surface wind stress $(\tilde{\tau}_1(\phi, \theta, \tilde{t}), \tilde{\tau}_2(\phi, \theta, \tilde{t}))$ is given in the following way:

$$\tilde{\tau}_1 = \tilde{\rho}\tilde{\nu}_1\frac{\partial \tilde{u}}{\partial \tilde{r}} \quad \text{on} \quad \tilde{r}(\phi, \theta, \tilde{t}) = \tilde{R} + \tilde{h}(\phi, \theta, \tilde{t}), \tag{2.8}$$

$$\tilde{\tau}_2 = \tilde{\rho}\tilde{\nu}_1\frac{\partial \tilde{v}}{\partial \tilde{r}} \quad \text{on} \quad \tilde{r}(\phi, \theta, \tilde{t}) = \tilde{R} + \tilde{h}(\phi, \theta, \tilde{t}). \tag{2.9}$$

This shows that solutions can be maintained by a fitting choice of vertical gradients. We assume the bottom of the ocean, where $\tilde{r} = \tilde{R} + \tilde{d}$, to be an solid impermeable stationary boundary. So we get the following conditions:

$$\tilde{u} = \tilde{v} = \tilde{w} = 0 \quad \text{on} \quad \tilde{r}(\phi, \theta) = \tilde{R} + \tilde{d}(\phi, \theta). \tag{2.10}$$

Before proceeding with dimensionless variables we redefine the pressure $\tilde{p}$:

$$\tilde{p} = \tilde{\rho}\left(-\tilde{g}\tilde{r} + \frac{\tilde{r}^2\tilde{\Omega}^2\cos^2\theta}{2}\right) + \tilde{P}(\phi, \theta, \tilde{r}, \tilde{t}). \tag{2.11}$$

[1]To be precise the earth is not a perfect sphere, it is an ellipsoid, but here it is enough to consider it as a sphere. For a more details on the exact form of the earth see the discussion in [25].

[2]The boundary is moving with the fluid, see [7].

2.2.2 Dimensional analysis

Now we non-dimensionalise:

$$\begin{aligned}\tilde{z} &= \tilde{D}z,\\ (\tilde{u},\tilde{v},\tilde{w}) &= \tilde{U}(u,v,\kappa w),\\ \tilde{P} &= \tilde{\rho}\tilde{U}^2 P,\\ \tilde{\nu}_1 &= \tilde{\nu}\hat{K}.\end{aligned} \tag{2.12}$$

The dimensional constant $\tilde{D}$ is an appropriate depth or height in which we are interested in[3], which will be chosen later; $\tilde{U}$ is a speed scale. The typical speed at the surface at mid-latitudes is 0.1m/s, see [8]. The constant κ is not chosen yet, but we predict it to be small, because there is weak vertical motion in these approximations (For more details on factors affecting vertical motion of the atmosphere see [27] and the ocean see [13]). For reducing (2.1), (2.2) and (2.3) we need a small parameter, which we choose to be:

$$\varepsilon = \frac{\tilde{D}}{\tilde{R}}. \tag{2.13}$$

We repeat $\tilde{R} \approx 6.378 \times 10^6$m and anticipate $\tilde{D} \approx 10^2$, hence $\varepsilon \approx 6 \times 10^{-4}$.
Before going back to Navier-Stokes equations we define:

$$\begin{aligned}\omega &= \frac{\tilde{\Omega}\tilde{R}}{\tilde{U}},\\ \mathfrak{R}_1 &= \frac{\tilde{U}\tilde{R}}{\tilde{\nu}},\\ \mathfrak{R}_2 &= \frac{\tilde{U}\tilde{R}}{\tilde{\nu}_2},\end{aligned} \tag{2.14}$$

where $\frac{1}{\omega}$ is the Rossby number and $(\mathfrak{R}_1, \mathfrak{R}_2)$ is the pair of Reynolds numbers. By combining (2.1), (2.2), (2.3) with (2.5), (2.11), (2.12), (2.13) and (2.14) we get the

[3] At most a few kilometers, i.e. something in the order of 10^3m. As seen in the introduction we will even only consider height at a few hundred meters, so something in the order of 10^2m.

following governing equations:

$$
\begin{aligned}
&\frac{u}{(1+\varepsilon z)\cos\theta}\frac{\partial u}{\partial \phi}+\frac{v}{1+\varepsilon z}\frac{\partial u}{\partial \theta}+\frac{\kappa w}{\varepsilon}\frac{\partial u}{\partial z}\\
&+\frac{1}{1+\varepsilon z}(-uv\tan\theta+\kappa uw)+2\omega(-v\sin\theta+\kappa w\cos\theta)\\
&=-\frac{1}{(1+\varepsilon z)\cos\theta}\frac{\partial P}{\partial \phi}+\frac{\hat{K}}{\mathfrak{R}_1}\left(\frac{1}{\varepsilon^2}\frac{\partial^2 u}{\partial z^2}+\frac{2}{\varepsilon(1+\varepsilon z)}\frac{\partial u}{\partial z}\right)\\
&+\frac{1}{\mathfrak{R}_2(1+\varepsilon z)^2}\left(\frac{1}{\cos^2\theta}\frac{\partial^2 u}{\partial \phi^2}-\tan\theta\frac{\partial u}{\partial \theta}+\frac{\partial^2 u}{\partial \theta^2}\right),
\end{aligned}
\tag{2.15}
$$

$$
\begin{aligned}
&\frac{u}{(1+\varepsilon z)\cos\theta}\frac{\partial v}{\partial \phi}+\frac{v}{1+\varepsilon z}\frac{\partial v}{\partial \theta}+\frac{\kappa w}{\varepsilon}\frac{\partial v}{\partial z}\\
&+\frac{1}{1+\varepsilon z}(u^2\tan\theta+\kappa vw)+2\omega u\sin\theta\\
&=-\frac{1}{1+\varepsilon z}\frac{\partial P}{\partial \theta}+\frac{\hat{K}}{\mathfrak{R}_1}\left(\frac{1}{\varepsilon^2}\frac{\partial^2 v}{\partial z^2}+\frac{2}{\varepsilon(1+\varepsilon z)}\frac{\partial v}{\partial z}\right)\\
&+\frac{1}{\mathfrak{R}_2(1+\varepsilon z)^2}\left(\frac{1}{\cos^2\theta}\frac{\partial^2 v}{\partial \phi^2}-\tan\theta\frac{\partial v}{\partial \theta}+\frac{\partial^2 v}{\partial \theta^2}\right),
\end{aligned}
\tag{2.16}
$$

$$
\begin{aligned}
&\frac{\kappa u}{(1+\varepsilon z)\cos\theta}\frac{\partial w}{\partial \phi}+\frac{\kappa v}{1+\varepsilon z}\frac{\partial w}{\partial \theta}+\frac{\kappa^2 w}{\varepsilon}\frac{\partial w}{\partial z}\\
&+\frac{1}{1+\varepsilon z}(-u^2-v^2)-2\omega u\cos\theta\\
&=-\frac{1}{\varepsilon}\frac{\partial P}{\partial z}+\frac{\hat{K}\kappa}{\mathfrak{R}_1}\left(\frac{1}{\varepsilon^2}\frac{\partial^2 w}{\partial z^2}+\frac{2}{\varepsilon(1+\varepsilon z)}\frac{\partial w}{\partial z}\right)\\
&+\frac{\kappa}{\mathfrak{R}_2(1+\varepsilon z)^2}\left(\frac{1}{\cos^2\theta}\frac{\partial^2 w}{\partial \phi^2}-\tan\theta\frac{\partial w}{\partial \theta}+\frac{\partial^2 w}{\partial \theta^2}\right).
\end{aligned}
\tag{2.17}
$$

In a similar fashion the equation of mass (2.4) combined with (2.11), (2.12), (2.13) and (2.14) becomes:

$$
\frac{1}{(1+\varepsilon z)\cos\theta}\left(\frac{\partial u}{\partial \phi}+\frac{\partial}{\partial \theta}(v\cos\theta)\right)+\frac{\kappa}{\varepsilon(1+\varepsilon z)^2}\frac{\partial}{\partial z}\left((1+\varepsilon z)^2 w\right)=0. \tag{2.18}
$$

We redefine $\kappa := \varepsilon k$, where k is to be chosen later. Furthermore, it is important to investigate into the viscous terms to make suitable and consistent choices with the underlying type of flow we investigate in. We take the term with the coefficient $1/(\varepsilon^2\mathfrak{R}_1)$ to be the dominant one. We now use this to define $\tilde{D}=\sqrt{\tilde{R}\tilde{\nu}_1/\tilde{U}}$. We treat ω to be of order 1 ($\omega \approx O(1)$). Hence, we could include it in the definition before and write:

$$\tilde{D} = \sqrt{\frac{\tilde{\nu}_1}{\tilde{\Omega}}}. \tag{2.19}$$

Using the above, we get an expression for the horizontal eddy viscosity:

$$\frac{1}{\mathfrak{R}_2} = \frac{\varepsilon\tilde{\nu}_2}{\tilde{\nu}_1} = \varepsilon^2\mu \quad \text{,where} \quad \mu = \frac{\tilde{\nu}_2}{\tilde{\nu}_1}. \tag{2.20}$$

We can quickly check that:

$$\frac{1}{\mathfrak{R}_1} = \varepsilon^2 \tag{2.21}$$

By taking equations (2.15), (2.16), (2.17), applying (2.20), (2.21), using $k\varepsilon$ instead of κ and multiplying the third equation with ε, we get:

$$\begin{aligned} &\frac{u}{(1+\varepsilon z)\cos\theta}\frac{\partial u}{\partial\phi} + \frac{v}{1+\varepsilon z}\frac{\partial u}{\partial\theta} + kw\frac{\partial u}{\partial z} \\ &+\frac{1}{1+\varepsilon z}(-uv\tan\theta + \varepsilon kuw) + 2\omega(-v\sin\theta + \varepsilon kw\cos\theta) \\ &= -\frac{1}{(1+\varepsilon z)\cos\theta}\frac{\partial P}{\partial\phi} + \hat{K}\left(\frac{\partial^2 u}{\partial z^2} + \frac{2\varepsilon}{(1+\varepsilon z)}\frac{\partial u}{\partial z}\right) \\ &+\frac{\varepsilon^2\mu}{(1+\varepsilon z)^2}\left(\frac{1}{\cos^2\theta}\frac{\partial^2 u}{\partial\phi^2} - \tan\theta\frac{\partial u}{\partial\theta} + \frac{\partial^2 u}{\partial\theta^2}\right), \end{aligned} \tag{2.22}$$

$$\begin{aligned} &\frac{u}{(1+\varepsilon z)\cos\theta}\frac{\partial v}{\partial\phi} + \frac{v}{1+\varepsilon z}\frac{\partial v}{\partial\theta} + kw\frac{\partial v}{\partial z} \\ &+\frac{1}{1+\varepsilon z}(u^2\tan\theta + \varepsilon kvw) + 2\omega u\sin\theta \\ &= -\frac{1}{1+\varepsilon z}\frac{\partial P}{\partial\theta} + \hat{K}\left(\frac{\partial^2 v}{\partial z^2} + \frac{2\varepsilon}{(1+\varepsilon z)}\frac{\partial v}{\partial z}\right) \\ &+\frac{\varepsilon^2\mu}{(1+\varepsilon z)^2}\left(\frac{1}{\cos^2\theta}\frac{\partial^2 v}{\partial\phi^2} - \tan\theta\frac{\partial v}{\partial\theta} + \frac{\partial^2 v}{\partial\theta^2}\right), \end{aligned} \tag{2.23}$$

$$
\begin{aligned}
\frac{u}{(1+\varepsilon z)\cos\theta}\frac{\partial \varepsilon^2 kw}{\partial \phi} + \frac{v}{1+\varepsilon z}\frac{\partial \varepsilon^2 kw}{\partial \theta} + kw\frac{\partial \varepsilon^2 kw}{\partial z} \\
+\frac{1}{1+\varepsilon z}(-\varepsilon u^2 - \varepsilon v^2) - 2\omega\varepsilon u\cos\theta \\
= -\frac{\partial P}{\partial z} + \hat{K}\left(\frac{\partial^2 \varepsilon^2 kw}{\partial z^2} + \frac{2\varepsilon}{(1+\varepsilon z)}\frac{\partial \varepsilon^2 kw}{\partial z}\right) \\
+\frac{\varepsilon^2\mu}{(1+\varepsilon z)^2}\left(\frac{1}{\cos^2\theta}\frac{\partial^2 \varepsilon^2 kw}{\partial \phi^2} - \tan\theta\frac{\partial \varepsilon^2 kw}{\partial \theta} + \frac{\partial^2 \varepsilon^2 kw}{\partial \theta^2}\right).
\end{aligned}
\tag{2.24}
$$

Again, doing the same with the dimensionless version of the equation of mass conservation yields:

$$
\frac{1}{(1+\varepsilon z)\cos\theta}\left(\frac{\partial u}{\partial \phi} + \frac{\partial}{\partial \theta}(v\cos\theta)\right) + \frac{k}{(1+\varepsilon z)^2}\frac{\partial}{\partial z}\left((1+\varepsilon z)^2 w\right) = 0. \tag{2.25}
$$

2.3 Linearization and f-plane approximation

Now we are interested in a system of equations, where μ, k, ω are fixed and $\varepsilon \to 0$. We now focus on (2.22), (2.23) and (2.24) with $k = O(1)$. In classical Ekman models, it is a standard condition, that the vertical velocity component is ignored, which is implied by $k = O(1)$. So (2.22),(2.23) and (2.24) become:

$$
\begin{aligned}
\left(\frac{u}{\cos\theta}\frac{\partial}{\partial \phi} + v\frac{\partial}{\partial \theta}\right)u - uv\tan\theta - 2\omega v\sin\theta \\
= -\frac{1}{\cos\theta}\frac{\partial P}{\partial \phi} + \hat{K}\frac{\partial^2 u}{\partial z^2},
\end{aligned}
\tag{2.26}
$$

$$
\begin{aligned}
\left(\frac{u}{\cos\theta}\frac{\partial}{\partial \phi} + v\frac{\partial}{\partial \theta}\right)v - u^2\tan\theta + 2\omega v\sin\theta \\
= -\frac{\partial P}{\partial \theta} + \hat{K}\frac{\partial^2 u}{\partial z^2},
\end{aligned}
\tag{2.27}
$$

$$
0 = -\frac{\partial P}{\partial z}. \tag{2.28}
$$

Next we linearize equations (2.26) and (2.27) to get:

$$
-2\omega v\sin\theta = -\frac{1}{\cos\theta}\frac{\partial P}{\partial \phi} + \hat{K}\frac{\partial^2 u}{\partial z^2}, \tag{2.29}
$$

$$
2\omega u\sin\theta = -\frac{\partial P}{\partial \theta} + \hat{K}\frac{\partial^2 u}{\partial z^2}, \tag{2.30}
$$

We utilize the classical used f-plane approximation, which means that $f := 2\omega \sin\theta =$ constant. We can heuristically imagine it like this: We say the Earth looks flat locally and treat it that way, but we still include Coriolis forces. For this adjustment it is required to perform a coordinate transform: $y = \theta$ and $x = \phi\cos\theta$. This results in:

$$-fv = -\frac{\partial P}{\partial x} + \hat{K}\frac{\partial^2 u}{\partial z^2}, \tag{2.31}$$

$$fu = -\frac{\partial P}{\partial y} + \hat{K}\frac{\partial^2 v}{\partial z^2}. \tag{2.32}$$

The next part follows [7] and [4]: We now assume a flow over a flat bottom. Using (2.10) and translating flat bottom to $d = 0$, this assumption gives our first boundary condition:

$$u = 0,\ v = 0 \text{ for } z = 0. \tag{2.33}$$

Moreover, we want to consider a spatially nonuniform interior flow, that is varying on a scale to be in geostrophic equilibrium with velocity u_g and v_g in $x-$ and $y-$ direction respectively. So for large z we have

$$u \approx u_g \text{ and } v \approx v_g. \tag{2.34}$$

or more mathematically:

$$\lim_{z\to\infty} u(z) = u_g, \lim_{z\to\infty} v(z) = v_g. \tag{2.35}$$

From equation (2.6) we conclude that the dimensionless pressure p is the same for all z. For spatially nonuniform interior flow we can use (2.35) to get from (2.31) and (2.32) the following equation:

$$fv_g = \frac{\partial P}{\partial x}. \tag{2.36}$$

$$fu_g = -\frac{\partial P}{\partial y}, \tag{2.37}$$

We finally insert equations (2.36) and (2.37) into (2.31) and (2.32) and get:

$$(v - v_g)f = -\hat{K}\frac{\partial^2 u}{\partial z^2}, \tag{2.38}$$

$$(u - u_g)f = \hat{K}\frac{\partial^2 v}{\partial z^2}. \tag{2.39}$$

2.4 Complex notation

We use complex variables by defining $\psi := u + iv$, $\psi_g := u_g + iv_g$ and re-scale the non-dimensional "viscosity" $K := \frac{2\hat{K}}{f}$ to rephrase the governing equations (2.38),(2.39) and its boundary conditions (2.33),(2.35) as follows:

$$K\psi'' - 2i(\psi - \psi_g) = 0 \tag{2.40}$$

$$\psi(0) = 0 \tag{2.41}$$

$$\lim_{z\to\infty} \psi(z) = \psi_g \tag{2.42}$$

For convenience we write a prime for the derivative.

3 The exact solution for the velocity components

In Ekman's paper [10] the function K is considered to be constant. Now we show a method to solve the equations above with K being a step function with finitely many steps, i.e. $K(z) = \sum_{n=0}^{N-1} l_n \mathbb{I}_{[a_n,a_{n+1})}(z)$, where $l_n \in \mathbb{R}^+ = \{x \in \mathbb{R} | x > 0\}$, $l_j \neq l_{j+1}$, for $j = 0, ..., N-2$, are constants, $a_n \in \mathbb{R}$, $a_0 = 0$, $a_n < a_{n+1}$ for $n = 1, 2, ..., N-1$ and $a_N = \infty$.

Remark 3.1. *In the case of non-constant eddy viscosity, the Navier-Stokes equations at the beginning look a bit different, see [6]. The procedure is similar and the resulting governing equation of motion in that case is:*

$$(K\psi')' - 2i(\psi - \psi_g) = 0.$$

3.1 Constructing the solution of the governing equations for constant eddy viscosity

Without loss of generality we let $K = 1$ in (2.40). The solution is the following:

$$\psi(z) = Ae^{(1+i)z} + Be^{-(1+i)z} + \psi_g. \tag{3.1}$$

The boundary condition (2.42) implies that $A = 0$, because $e^{(1+i)z}$ is growing exponentially. From (2.41) we get $B = -\psi_g$. Hence, the solution is

$$\psi(z) = -\psi_g e^{-(1+i)z} + \psi_g. \tag{3.2}$$

3.2 Constructing the solution of the governing equations for piecewise uniform eddy viscosity

The next best thing to do is to regard the eddy viscosity as a step function with only one jump. W.l.o.g.:

$$K(z) = 1 \text{ ,for } \; 0 \leq z < h,$$

$$K(z) = l^2 \text{ ,for } \; h \leq z < \infty.$$

By defining K like this, (2.38) can be written as follows:

$$\psi'' - 2i(\psi - \psi_g) = 0 \text{ for } 0 \leq z < h, \tag{3.3}$$

$$l^2\psi'' - 2i(\psi - \psi_g) = 0 \text{ for } h \leq z < \infty. \tag{3.4}$$

Solving this well-known non-homogeneous linear differential equation of second order yields the solution:

$$\psi(z) = Ae^{(1+i)z} + Be^{-(1+i)z} + \psi_g \text{ for } 0 \leq z < h, \tag{3.5}$$

$$\psi(z) = Ce^{\frac{(1+i)z}{l}} + De^{-\frac{(1+i)z}{l}} + \psi_g \text{ for } h \leq z < \infty, \tag{3.6}$$

For finding explicit values for A, B, C and D, we first look at the boundary conditions (2.41) and (2.42). The latter implies, that

$$C = 0, \tag{3.7}$$

because $e^{(((1+i)z)/l)}$ is a exponentially growing term. The first one of the boundary conditions directly gives:

$$A + B + \psi_g = 0. \tag{3.8}$$

Next, we assume continuity of ψ, so $\psi(h^-) = \psi(h^+)$. Inserting and equalizing (3.5) and (3.6) results in:

$$Ae^{(1+i)h} + Be^{-(1+i)h} = De^{-\frac{(1+i)h}{l}}. \tag{3.9}$$

Finally, we use again the continuity of ψ and additionally integrate (3.3) and (3.4) over an infinitesimal region with center $z = h$:

$$\psi'(h^-) = l^2\psi'(h^+). \tag{3.10}$$

Inserting yields:

$$Ae^{(1+i)h} - Be^{-(1+i)h} = -lDe^{-\frac{(1+i)h}{l}}. \tag{3.11}$$

By (3.8), (3.9), (3.11) and (3.7) (in this particular order), we create the following system of equations:

$$\begin{bmatrix} 1 & 1 & 0 & 0 \\ e^{(1+i)h} & e^{-(1+i)h} & -e^{-\frac{(1+i)h}{l}} & 0 \\ e^{(1+i)h} & -e^{-(1+i)h} & le^{-\frac{(1+i)h}{l}} & 0 \\ 0 & 0 & 0 & 1 \end{bmatrix} \begin{pmatrix} A \\ B \\ D \\ C \end{pmatrix} = \begin{pmatrix} -\psi_g \\ 0 \\ 0 \\ 0 \end{pmatrix}, \tag{3.12}$$

Solving the above gives:

$$A = \frac{\psi_g(l-1)}{1 + e^{(2+2i)h} - l + e^{(2+2i)h}l}, \tag{3.13}$$

$$B = -\frac{\psi_g e^{(2+2i)h}(l+1)}{1 + e^{(2+2i)h} - l + e^{(2+2i)h}l}, \tag{3.14}$$

$$C = 0 \tag{3.15}$$

$$D = -\frac{2\psi_g e^{(1+i)h+\frac{(1+i)h}{l}}}{1 + e^{(2+2i)h} - l + e^{(2+2i)h}l}. \tag{3.16}$$

Hence, equation (3.3),(3.4) is fully solved for $K(z) = 1$ for $0 \leq z < h$ and $K(z) = l^2$ for $h \leq z < \infty$.

3.3 Constructing the solution of the governing equations for general piecewise uniform eddy viscosity

In the general case, we set $K(z) = \sum_{n=0}^{N-1} l_n^2 \mathbb{I}_{[a_n,a_{n+1})}(z)$, where $l_n \in \mathbb{R}^+ = \{x \in \mathbb{R} | x > 0\}$, $l_j \neq l_{j+1}$, for $j = 1, 2, ..., N-2$; $a_0 = 0$, $a_n \in \mathbb{R}$, $a_n < a_{n+1}$ for $n = 1, 2, ..., N-1$ and $a_N = \infty$. Hence, the equation (2.40) can be written in the following way:

$$\begin{aligned} l_0^2\psi'' - 2i(\psi - \psi_g) &= 0 \text{ for } a_n = 0 \leq z < a_1, \\ l_1^2\psi'' - 2i(\psi - \psi_g) &= 0 \text{ for } a_1 \leq z < a_2, \\ &\vdots \\ l_{N-1}^2\psi'' - 2i(\psi - \psi_g) &= 0 \text{ for } a_{N-1} \leq z < a_N = \infty. \end{aligned} \tag{3.17}$$

Using the same solving method as above, we have $2N$ instead of four unknown constants. The solved equations with still to calculate coefficients look like this:

$$\begin{aligned} \psi(z) &= A_{0,0}e^{\frac{(1+i)z}{l_0}} + A_{0,1}e^{-\frac{(1+i)z}{l_0}} + \psi_g \text{ for } a_0 = 0 \leq z < a_1, \\ \psi(z) &= A_{1,0}e^{\frac{(1+i)z}{l_1}} + A_{1,1}e^{-\frac{(1+i)z}{l_1}} + \psi_g \text{ for } a_1 \leq z < a_2, \\ &\vdots \\ \psi(z) &= A_{N-1,0}e^{\frac{(1+i)z}{l_{N-1}}} + A_{N-1,1}e^{-\frac{(1+i)z}{l_{N-1}}} + \psi_g \text{ for } a_{N-1} \leq z < \infty. \end{aligned} \tag{3.18}$$

The two boundary conditions (2.41) and (2.42) again imply respectively:

$$A_{0,0} + A_{0,1} + \psi_g = 0, \tag{3.19}$$

$$A_{N-1,1} = 0, \tag{3.20}$$

By imposing continuity on ψ we get the following $N-1$ conditions:

$$\begin{aligned} A_{0,0}e^{\frac{(1+i)a_1}{l_0}} + A_{0,1}e^{-\frac{(1+i)a_1}{l_0}} &= A_{1,0}e^{\frac{(1+i)a_1}{l_1}} + A_{1,1}e^{-\frac{(1+i)a_1}{l_1}}, \\ A_{1,0}e^{\frac{(1+i)a_2}{l_1}} + A_{1,1}e^{-\frac{(1+i)a_2}{l_1}} &= A_{2,0}e^{\frac{(1+i)a_2}{l_2}} + A_{2,1}e^{-\frac{(1+i)a_2}{l_2}}, \\ &\vdots \\ A_{N-2,0}e^{\frac{(1+i)a_{N-1}}{l_{N-2}}} + A_{N-2,1}e^{-\frac{(1+i)a_{N-1}}{l_{N-2}}} &= A_{N-1,0}e^{\frac{(1+i)a_{N-1}}{l_{N-1}}}. \end{aligned} \tag{3.21}$$

We then integrate the equations (3.17) over an infinitesimal region with the center being the discontinuities of K, namely the a_n, $n = 1, 2, ..., N-1$. This yields:

$$\begin{aligned} l_0^2\psi'(a_1^-) &= l_1^2\psi'(a_1^+), \\ l_1^2\psi'(a_2^-) &= l_2^2\psi'(a_2^+), \\ &\vdots \\ l_{N-2}^2\psi'(a_{N-1}^-) &= l_{N-1}^2\psi'(a_{N-1}^+). \end{aligned} \tag{3.22}$$

Finally, the conditions above on ψ' at $z = a_n, n = 1, 2, ..., N-1$ immediately imply:

$$\begin{aligned} l_0 A_{0,0} e^{\frac{(1+i)a_1}{l_0}} - l_0 A_{0,1} e^{-\frac{(1+i)a_1}{l_0}} &= l_1 A_{1,0} e^{\frac{(1+i)a_1}{l_1}} - l_1 A_{1,1} e^{-\frac{(1+i)a_1}{l_1}}, \\ l_1 A_{1,0} e^{\frac{(1+i)a_2}{l_1}} - l_1 A_{1,1} e^{-\frac{(1+i)a_2}{l_1}} &= l_2 A_{2,0} e^{\frac{(1+i)a_2}{l_2}} - l_2 A_{2,1} e^{-\frac{(1+i)a_2}{l_2}}, \\ &\vdots \\ l_{N-2} A_{N-2,0} e^{\frac{(1+i)a_{N-1}}{l_{N-2}}} - l_{N-2} A_{N-2,1} e^{-\frac{(1+i)a_{N-1}}{l_{N-2}}} &= l_{N-1} A_{N-1,0} e^{\frac{(1+i)a_{N-1}}{l_{N-1}}}. \end{aligned} \tag{3.23}$$

The equations (3.19), (3.20), (3.21) and (3.23) are $1 + 1 + (N-1) + (N-1) = 2N$ linear equations for $2N$ unknown constants. They are all obviously linear independent. Hence, we can generate a solution by solving the following problem:

$$\mathcal{M}\mathbf{A} = \mathbf{b}, \tag{3.24}$$

with $\alpha_n := e^{\frac{(1+i)a_{n+1}}{l_n}}$, $\beta_n := e^{\frac{(1+i)a_n}{l_n}}$, $\hat{\alpha}_n = (\alpha_n, \alpha_n)$, $\hat{\beta}_n = (\beta_n, \beta_n)$, $\check{\alpha}_n = (\alpha_n, -\alpha_n)$, $\check{\beta}_n = (\beta_n, -\beta_n)$, $n = 0, 1, 2, ..., N-1$, $\mathbf{1} = (1, 1)$, $\hat{\mathbf{1}} = (0, 1)$;

$$\mathcal{M} =$$

$$\begin{bmatrix} \mathbf{1} & 0 & 0 & \cdots & 0 \\ \hat{\alpha}_0 & -\hat{\beta}_1 & 0 & \ddots & 0 \\ 0 & \hat{\alpha}_1 & -\hat{\beta}_2 & \ddots & 0 \\ \vdots & \ddots & \ddots & \ddots & \vdots \\ 0 & 0 & \cdots & \hat{\alpha}_{N-2} & -\hat{\beta}_{N-1} \\ l_0\check{\alpha}_0 & -l_1\check{\beta}_1 & 0 & \cdots & 0 \\ 0 & l_1\check{\alpha}_1 & -l_2\check{\beta}_2 & \ddots & 0 \\ \vdots & \ddots & \ddots & \ddots & \vdots \\ 0 & 0 & \cdots & l_{N-2}\check{\alpha}_{N-2} & -l_{N-1}\check{\beta}_{N-1} \\ 0 & 0 & \cdots & 0 & \hat{\mathbf{1}} \end{bmatrix},$$

$$\mathbf{A} = (A_{0,0}, A_{0,1}, A_{1,0}, A_{1,1}, ..., A_{N-1,0}, A_{N-1,1})^T,$$

$$\mathbf{b} = (-\psi_g, 0, ..., 0)^T.$$

The variable $\mathcal{M}$ is a $2N \times 2N$-Matrix, which is written in block-matrix form; $\mathbf{A}$ and $\mathbf{b}$ are vectors with $2N$ entries. To clarify the matrix: The first row comes from (3.19), the second to the N-th row from (3.21), the $N+1$-th to the $2N-1$-th row from (3.23) and the last row from (3.20). All in all solving the problem (3.18) and inserting the values for $A_{i,j}$, $i = 1, 2, ..., N-1; j = 1, 2$ into the equations (3.12) gives an explicit solution to the boundary value problem (3.11).

Remark 3.2. *In the equations* (3.9),(3.11) *and* (3.21), (3.23) *we already inserted* $C = 0$ *and* $A_{N-1,1} = 0$ *respectively. In particular the last row and the very right column of the matrices in* (3.12) *and* (3.24) *are redundant, when calculating, but we keep it for visualization reasons.*

In the next chapters we only regard the simpler cases, where $N = 1$ and $N = 2$, because calculating the upcoming results works for every finite N very similarly.

4 The Ekman spiral

We define the angle γ between the wind at any height and that of the geostrophic vector in the same manner as in the paper [4].

$$\tan(\gamma(z)) = \frac{\Im\left(\frac{\psi(z)}{\psi_g}\right)}{\Re\left(\frac{\psi(z)}{\psi_g}\right)}. \tag{4.1}$$

In particular we calculate the angle between the surface wind and that of the geostrophic vector. After inserting $\psi(0)$ into (4.1), we see from the initial condition (2.41) that

$$\lim_{z\to 0} \frac{\Im\left(\frac{\psi(z)}{\psi_g}\right)}{\Re\left(\frac{\psi(z)}{\psi_g}\right)} = \frac{0}{0}, \tag{4.2}$$

which is not defined. Hence we apply L'Hospital's rule. This means

$$\lim_{z\to 0} \frac{\Im\left(\frac{\psi(z)}{\psi_g}\right)}{\Re\left(\frac{\psi(z)}{\psi_g}\right)} = \lim_{z\to 0} \frac{\Im\left(\frac{\psi(z)}{\psi_g}\right)'}{\Re\left(\frac{\psi(z)}{\psi_g}\right)'}. \tag{4.3}$$

4.1 An exact formula for the Ekman spiral for constant eddy visosity

We continue with equation (3.2) and try to insert in (4.1) for the angle $\gamma_0 := \gamma(0)$. Making use of the needed L'Hospital's rule yields

$$\tan(\gamma_0) = 1, \tag{4.4}$$

which corresponds $\gamma_0 = 45°$, hence Ekman's result. The angle for $z > 0$ can be attained by straight up inserting ψ form (3.2) into the above equation (4.1):

$$\tan(\gamma(z)) = \frac{\sin(z)}{e^z - \cos(z)}. \tag{4.5}$$

.

4.2 An exact formula for the Ekman spiral for non-uniform eddy visosity

We again assume the eddy viscosity to only have one jump, therefore we continue with ψ from (3.5) and (3.6) with solved coefficients. We can immediately check that $\psi'(0) = (1+i)(A-B)$. Inserting this into (4.3) and rewriting $e^{i\theta} = \cos(\theta) + i\sin(\theta)$ for $\theta \in \mathbb{R}$, we get

$$\tan(\gamma_0) = \frac{\alpha^2 - \beta^2 + 2\alpha\beta\sin(2h)}{\alpha^2 - \beta^2 - 2\alpha\beta\sin(2h)}, \tag{4.6}$$

where $\alpha := (1+l)e^h$ and $\beta := (1-l)e^{-h}$.

The deflection angle γ is well defined for $z > 0$ and can be calculated directly:

$$\tan(\gamma(z)) = \frac{\zeta_1(z)}{\nu_1(z)}, \text{ for } 0 < z < h, \text{ where} \tag{4.7}$$

$$\begin{aligned}\zeta_1(z) = &-e^{2h}\left(-1+e^{2z}\right)\left(-1+l^2\right)\sin(2h-z)\\ &+\left(-e^{2z}(-1+l)^2 + e^{4h}(1+l)^2\right)\sin(z),\end{aligned} \tag{4.8}$$

$$\begin{aligned}\nu_1(z) = &\, e^{2h}\left(-1+l^2\right)\left(-2e^z\cos(2h) + \left(1+e^{2z}\right)\cos(2h-z)\right)\\ &+e^{4h}(1+l)^2\left(e^z - \cos(z)\right) - e^z(-1+l)^2\left(-1+e^z\cos(z)\right);\end{aligned} \tag{4.9}$$

$$\tan(\gamma(z)) = \frac{\zeta_2(z)}{\nu_2(z)}, \text{ for } h \le z < \infty, \text{ where} \tag{4.10}$$

$$\begin{aligned}&\zeta_2(z) =\\ 2e^{h+\frac{h}{l}}&\left((-1+l)\sin\left(\frac{h+hl-z}{l}\right) + e^{2h}(1+l)\sin\left(\frac{-h+hl+z}{l}\right)\right)\end{aligned} \tag{4.11}$$

$$\begin{aligned}&\nu_2(z) = e^{\frac{z}{l}}\left((-1+l)^2 + e^{4h}(1+l)^2\right)\\ -2e^{2h+\frac{z}{l}}&\left(-1+l^2\right)\cos(2h) + 2e^{h+\frac{h}{l}}(-1+l)\cos\left(\frac{h+hl-z}{l}\right)\\ &-2e^{h\left(3+\frac{1}{l}\right)}(-1+l)\cos\left(\frac{-h+hl+z}{l}\right).\end{aligned} \tag{4.12}$$

Remark 4.1. *: By taking equation* (3.6) *and setting l=1, we get exactly the same solution for the Ekman Spiral, as if we start with equation* (3.1) *right away.*

Proof. We insert $l = 1$ into (3.13) through (3.16) and immediately get $A = 0$, $B = -\psi_g$ and $D = -\psi_g$, which corresponds to (3.2); Or we insert $l = 1$ into the formula (4.7) through (4.12) and get $\tan(\gamma_0) = 1$ and $\tan(\gamma(z)) = \frac{\sin(z)}{e^z - \cos(z)}$, which is literally (4.4) and (4.5) respectively. □

Remark 4.2. *: In the paper [9] from Dritschel, Paldor and Constanin the procedure is similar. The difference in [9] is, that the case under the ocean-surface is dealt with and hence they started with a different differential equation and boundary conditions, i.e.* $K\psi'' - 2i\psi = 0, \psi'(0) = 1, \lim_{z\to-\infty} \psi = 0$*. But we end up with exactly the same formula for the angle on the surface. In particular interpretations and behaviour found in that paper can be applied to this case. Nevertheless, we still examine some analytic properties. In the next chapter we use this and we will also see a quick derivation of the equations of motion for constant eddy viscosity.*

5 Interpretations

In the following we choose values for the nondimensional eddy viscosity K. They are not taken from real life measurements. However they are somehow in the order of the values found in [24] and [4].

We begin with graphs, that just shows the behaviour of the angle in terms of growth and decay. At the end we see a 3d model of how the currents are changing with respect to height, see figure 12.

5.1 The deflection angle

For the Ekman spiral we first look at Ekman's solution (4.5), the one with constant eddy viscosity, see figure 3. The angle between the surface wind and that of the geostrophic vector is $\gamma(0) = \gamma_0 \approx 0.785$, which corresponds to $\pi/4 = 45°$. Since we look at the angle between two complex numbers and the complex geostrophic wind component ψ_g is constant, the height dependent function ψ must turn to the right (clockwise) with increasing height z.

Next, we compare the above result to the height dependent angle $\gamma(z)$ from (4.6) with fixed value $l = 0.08$ ($K = 0.0064$), but different values for h.
In figure 4, we again observe that the angle between the wind at height z and that of the

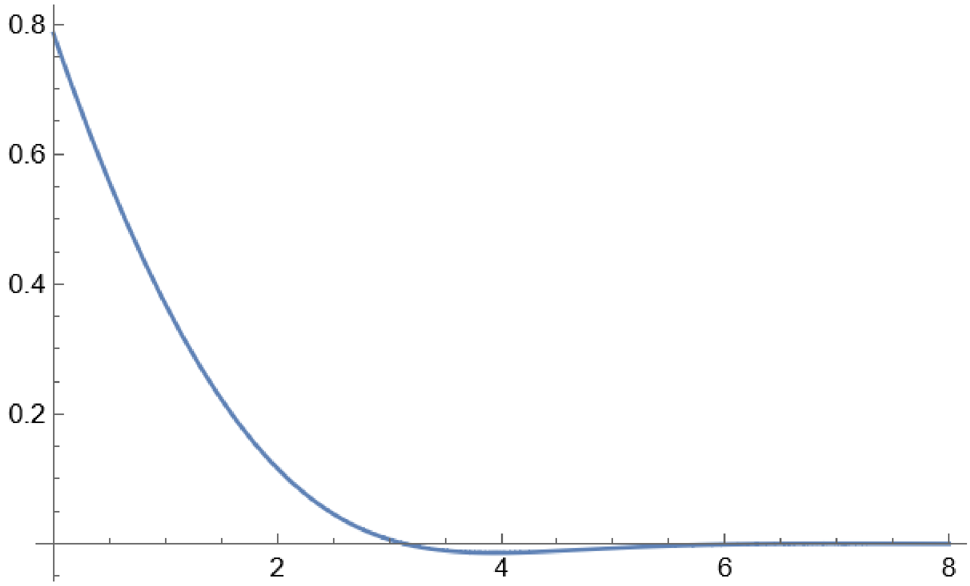

Figure 3: The vertical axis corresponds to $\gamma(z)$ and the horizontal one to z. This means this graph shows the behaviour of the angle between the wind at height z and that of the geostrophic vector with constant eddy viscosity $l = 1$ depending on height.

geostrophic vector is again about 45°, but at the change of viscosities the angle behaves differently.

Decreasing the change of viscosites further to $h = 2$, also decreases the deflection angle and we see that it can indeed attain values under 45°. In figure 5 we can see that the value on the vertical axis is just under 0.785, hence under 45°.

Decreasing h further, changes the angle to a value way over 45° as we see in figure 6.

To get an idea why the angle can have values much larger and just a bit smaller than 45°, we refer to the ”Analytic properties”-subsection. However we still graph the angle between the surface wind and that of the geostrophic vector depending on the change of eddy viscosity h, see figure 7.

Let us now assume that the eddy viscosity is larger. We set $l = 5$ and the change of eddy viscosity $h = 0.35$, see figure 8. We observe that the angle can indeed be much smaller, than 45°. The corresponding $(\gamma_0(h), h)$-graph is shown in figure 9.

5.2 Analytic properties

First, it can be observed in figure 7, 9 that for ”large” h the angle goes to 45°, which makes sense, since on the right hand side of equation (4.6) the exponential term e^h in the numerator as well as in the denominator keeps growing exponentially. The term

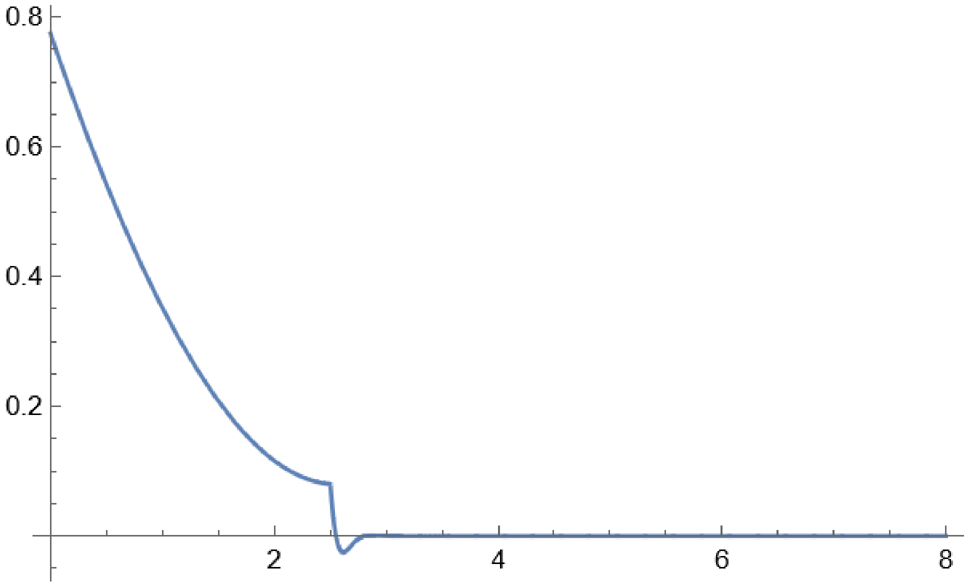

Figure 4: The vertical axis corresponds to $\gamma(z)$ and the horizontal one to z. The eddy viscosities are $l = 1$ and $l = 0.08$. The change of the eddy viscosity is $h = 2.5$.

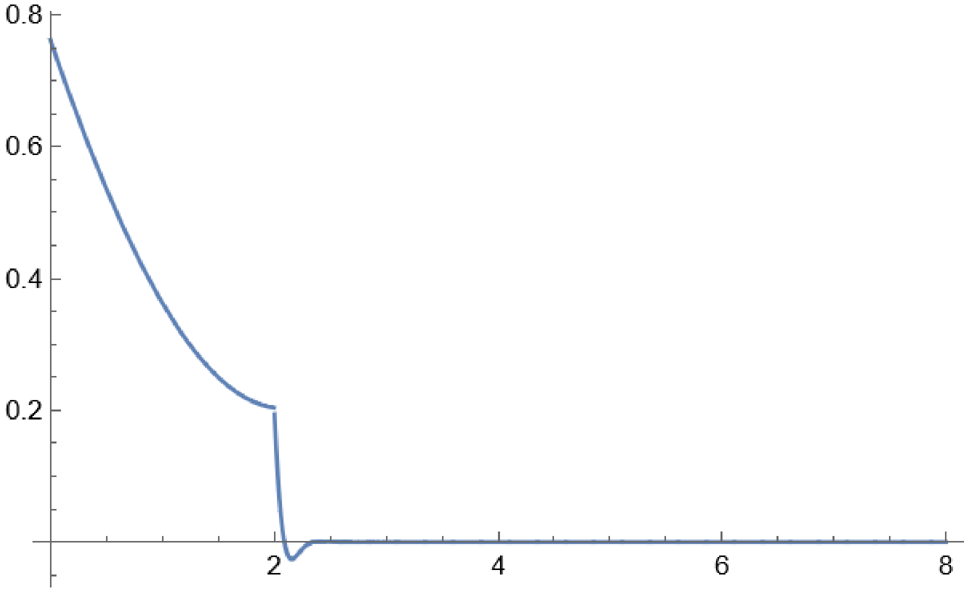

Figure 5: The vertical axis corresponds to $\gamma(z)$ and the horizontal one to z. The eddy viscosities are $l = 1$ and $l = 0.08$. The change of the eddy viscosity is $h = 2$.

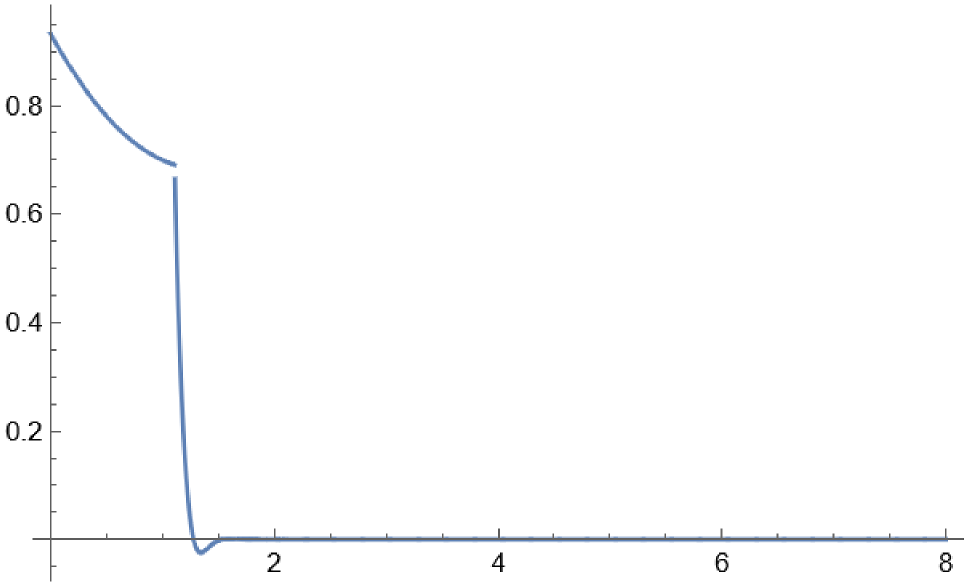

Figure 6: The vertical axis corresponds to $\gamma(z)$ and the horizontal one to z. The eddy viscosities are $l = 1$ and $l = 0.08$. The change of the eddy viscosity is $h = 1.1$.

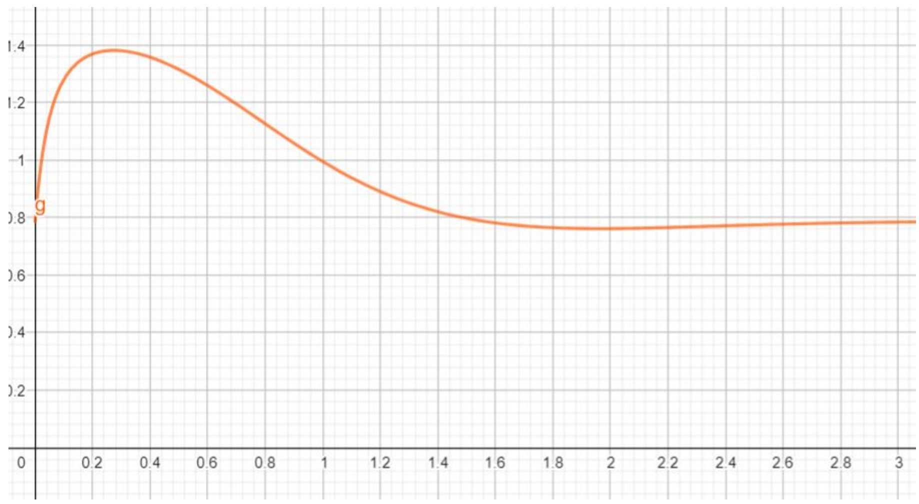

Figure 7: The constant $l = 0.08$. The vertical axis is the angle γ_0. The horizontal axis is the change of eddy viscosity h. For "small" h the angle is over $0.786 \approx \pi/4 = 45°$ and around $h = 2$ the deflection angle is just under $45°$.

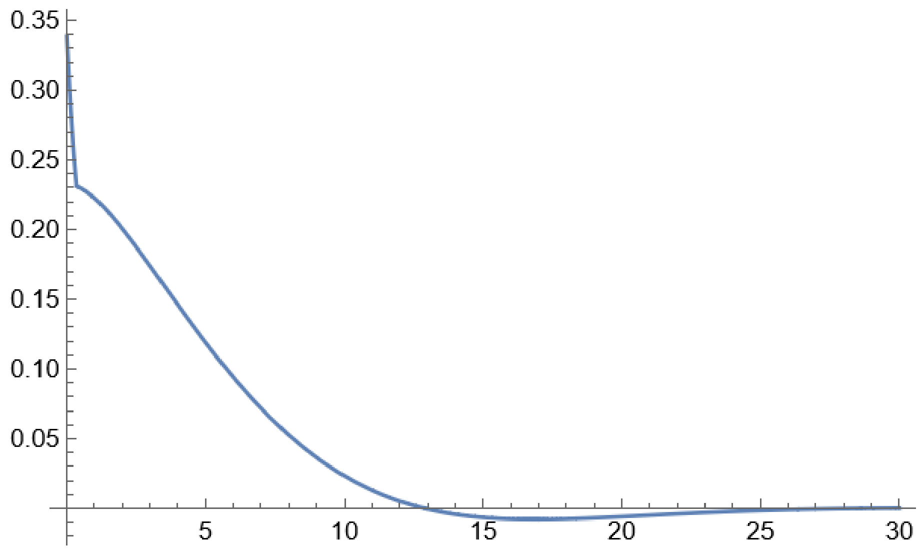

Figure 8: The vertical axis corresponds to $\gamma(z)$ and the horizontal one to z. The eddy viscosities are $l = 1$ and $l = 5$. The change of the eddy viscosity is $h = 0.35$.

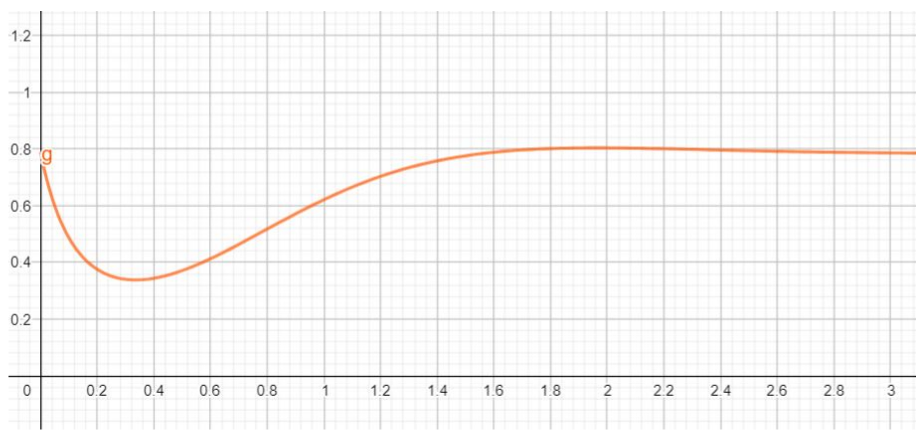

Figure 9: The constant $l = 5$. The vertical axis is the angle γ_0. The horizontal axis is the change of eddy viscosity h. For "small" h the angle is under $0.786 \approx \pi/4 = 45°$ and around $h = 2$ the deflection angle is just over $45°$.

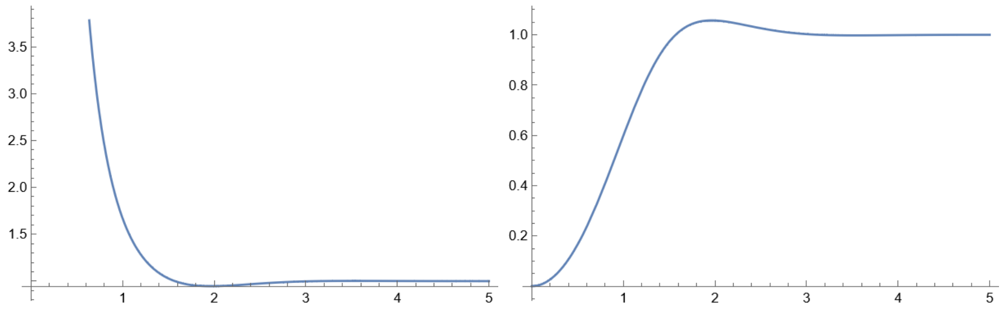

Figure 10: The vertical axis represents the angle between the surface wind and that of the geostrophic vector γ_0. The horizontal axis represents the change of eddy viscosity h. 1.Subgraph: The upper layer eddy viscosity is vanishing ; 2.Subgraph: The upper layer eddy viscosity is going to infinity.

e^{-h} becomes small and insignificant fast. The last term can be bounded by a constant: $|2\alpha\beta\sin(2h)| < 2|(1-l^2)|$, since $\alpha\beta = (1-l^2)$. With growing h the equation (4.6) becomes very quickly:

$$\tan(\gamma_0) \approx \frac{e^h}{e^h} = 1 \Rightarrow \gamma_0 \approx 45°. \tag{5.1}$$

Next, we can look what happens to the angle between the surface wind and that of the geostrophic vector, when $l \to 0$: The equation (4.6) becomes:

$$\tan(\gamma_0) = \frac{\sinh(2h) + \sin(2h)}{\sinh(2h) - \sin(2h)}, \tag{5.2}$$

see the first graph in figure 10. As $h \to 0$, it holds that $\tan(\gamma_0) \to \infty$, which corresponds to $\gamma_0 \to 90°$. For $l \to \infty$, the equation (4.6) becomes:

$$\tan(\gamma_0) = \frac{\sinh(2h) - \sin(2h)}{\sinh(2h) + \sin(2h)}, \tag{5.3}$$

see the second graph in figure 10. Here the "opposite" occurs: As $h \to 0$, where the minimum is, $\tan(\gamma_0) \to 0$, which corresponds to $\gamma_0 = 0°$.

5.3 The derivative

Now we calculate the derivative of the equation (4.1) and look at its graph, see figure 11. We observe that an obvious discontinuity occurs, which is expected from the assumptions that K is a step function.

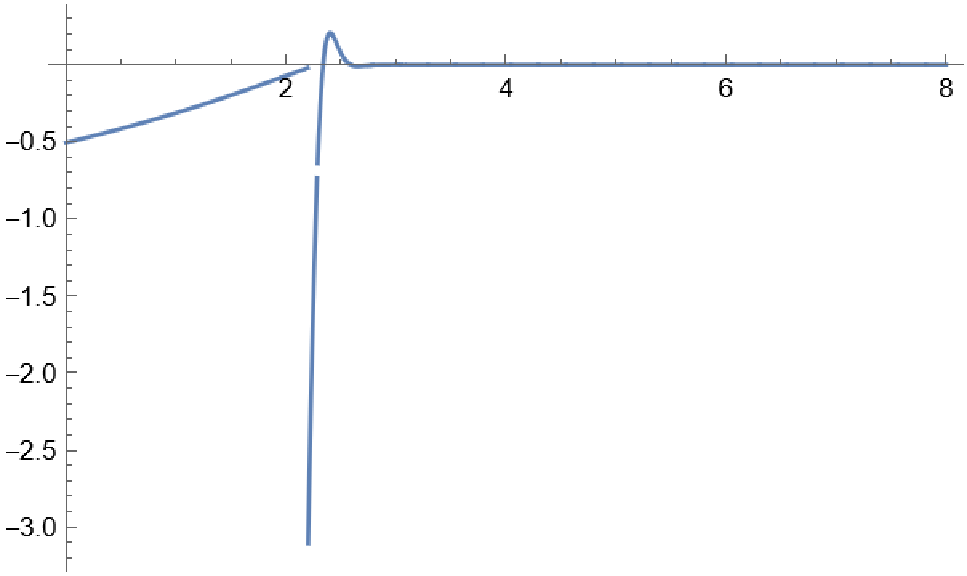

Figure 11: The vertical axis represents the derivative of γ. The horizontal axis represents the height z. We set $h = 2.2$ and $l = 0.08$. We observe, that γ is not continuous at the change of eddy viscosity h.

5.4 Oceanic and atmospheric Ekman spiral

Next, we want to compare the Ekman spiral over and under the surface. We shortly derive the Ekman spiral under the water. The equation of motions (2.31) and (2.32) are the same. A difference is that

$$\frac{\partial P}{\partial x} = 0, \ \frac{\partial P}{\partial y} = 0, \tag{5.4}$$

Inserting in (2.31) and (2.32), setting $2\hat{K}/f = k^2$ and using complex notion yields:

$$k^2\psi'' - 2i\psi = 0, \tag{5.5}$$

The initial conditions also have to be adapted (for details see [9], [7], [16]):

$$\psi'(0) = 1, \ \lim_{z \to -\infty} \psi = 0. \tag{5.6}$$

We solve equation (5.5):

$$\psi(z) = Ae^{\frac{(1+i)z}{k}} + Be^{-\frac{(1+i)z}{k}}. \tag{5.7}$$

We note that $z \leq 0$ here. The initial conditions imply that $B = 0$ for the same reason as before and $A = k/(1+i)$. The deflection angle is determined in the following way:

$$\tan(\delta(z)) = -\frac{\Im(\psi(z))}{\Re(\psi(z))} \tag{5.8}$$

We again observe that:

$$\tan(\delta_0) = -\frac{\Im(\psi(z))}{\Re(\psi(z))} = -\frac{\Im(A)}{\Re(A)} = -\frac{-\frac{k}{2}}{\frac{k}{2}} = 1 \Rightarrow \delta_0 = 45°.$$

In particular inserting the solved equation (5.7) into (5.8) yields:

$$\tan(\delta(z)) = \frac{\cos(\frac{z}{k}) - \sin(\frac{z}{k})}{\cos(\frac{z}{k}) + \sin(\frac{z}{k})}. \tag{5.9}$$

Of course we can now do the same as before for the case under the surface, by splitting the eddy viscosity into two, but exactly this is already done in [9].
We compare the the Ekman Spiral over and under the surface in figure 12. For positive z we use (4.4) and for negative z (5.9). We set the eddy viscosity constant $= 1$. The turning speed of the angle does not necessarily represent real life scenarios, but the direction in which the angle turns does, which is the aspect we focus on in this section. We observe that the angle is turning to the right (clockwise) going up as well as going down.

6 Conclusion

Motivated by Ekman's work in 1905 [10] and the recent papers [9] and [4], we first derived well-known equations of motion for mesoscale steady flow in the Ekman layer in non-equatorial regions of the northern hemisphere. We then assumed the eddy viscosity to be a step function. In addition to well-known boundary conditions we "found" new conditions to be able to exactly solve the equations of motion with non-uniform eddy viscosity. In particular we wrote up a method to solve these equations in a as general way as possible[4]. We then calculated a formula to the Ekman spiral and took a good look at the angle between the surface wind and that of the geostrophic vector. We first fixed the upper layer eddy viscosity l at a small and large value and investigated in the height $z = h$, where the eddy viscosity changes. We observed that angles over and under

[4]Here we mean, that the eddy viscosity can be any step function.

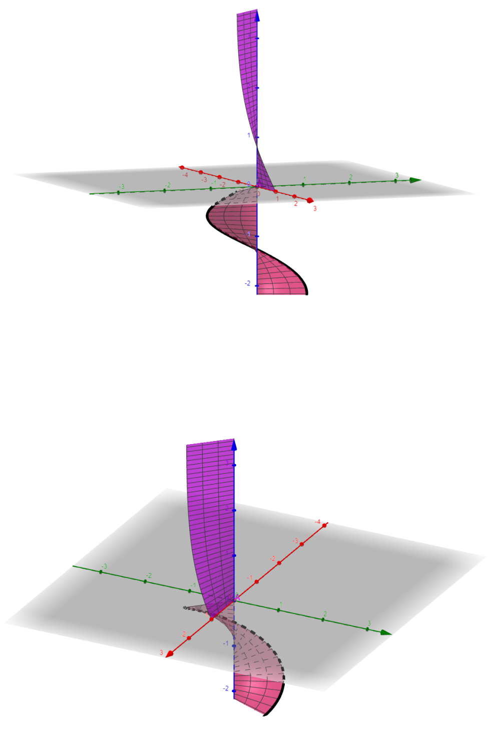

Figure 12: The surface wind is set along the red axis. The currents are represented by the black lines in the violet and red surfaces, that are parallel to the ground surface. Starting at the ground surface the angle is turning clockwise going up as well as going down.

45° can indeed occur. Next we extremized the problem by letting l going to zero and infinity and saw that for small h the angles range from $0^\circ - 90^\circ$. The highest and lowest angles are most likely not going to occur in the real world, nevertheless we get an insight on some influences on the angle.

References

[1] B.W. Berger and B. Grisogono. "The Baroclinic, Variable eddy Viscosity Ekman Layer". In: *Boundary-Layer Meteorology* 87 (1998), pp. 363–380.

[2] G. von Bogusławski and J.G.O. Krümmel. *Handbuch der Ozeanographie, von G. von Boguslawski (und O. Krümmel).* Bibl. geogr. Handbücher. 1884. URL: https://books.google.at/books?id=hP4HAAAAQAAJ.

[3] T. Chai, C.-L. Lin, and R. K. Newsom. "Retrieval of Microscale Flow Structures from High-Resolution Doppler Lidar Data Using an Adjoint Model." In: *Journal of Atmospheric Sciences* 61.13 (2004), pp. 1500–1520.

[4] A. Constantin and R.S. Johnson. "Atmospheric Ekman Flows with Variable eddy Viscosity". In: *Boundary-layer meteorology* 170.3 (2019), pp. 395–414.

[5] A. Constantin and R.S. Johnson. "Ekman-type solutions for shallow-water flows on a rotating sphere: A new perspective on a classical problem". In: *Physics of Fluids* 31 (2019), p. 021401.

[6] A. Constantin and R.S. Johnson. "Large-scale oceanic currents as shallow-water asymptotic solutions of the Navier-Stokes equation in rotating spherical coordinates". In: *Deep Sea Research Part II: Topical Studies in Oceanography* 160 (2019). Waves and Currents, pp. 32–40. URL: https://www.sciencedirect.com/science/article/pii/S0967064518301814.

[7] B. Cushman-Roisin and J.M. Beckers. *Introduction to Geophysical Fluid Dynamics: Physical and Numerical Aspects.* International Geophysics. Elsevier Science, 2011. URL: https://books.google.at/books?id=3KS8sD5ky9kC.

[8] H.A. Dijkstra. *Nonlinear Physical Oceanography: A Dynamical Systems Approach to the Large Scale Ocean Circulation and El Niño.* Atmospheric and Oceanographic Sciences Library. Springer Netherlands, 2013. URL: https://books.google.at/books?id=glHqCAAAQBAJ.

[9] D.G. Dritschel, N. Paldor, and A. Constantin. "The Ekman spiral for piecewise-uniform viscosity". In: *Ocean Science* 16.5 (2020), pp. 1089–1093. URL: https://os.copernicus.org/articles/16/1089/2020/.

[10] V.W. Ekman. "On the influence of the earth's rotation on ocean-currents". In: *Ark. Mat. Astron. Fys.* 1905, pp. 1–52.

[11] M.A. Estoque. “A numerical model of the atmospheric boundary layer”. In: *Journal of Geophysical Research (1896-1977)* 68.4 (1963), pp. 1103–1113. eprint: https://agupubs.onlinelibrary.wiley.com/doi/pdf/10.1029/JZ068i004p01103. URL: https://agupubs.onlinelibrary.wiley.com/doi/abs/10.1029/JZ068i004p01103.

[12] F. Fleming. *Ninety Degrees North: The Quest For The North Pole*. Granta Publications, 2011. URL: https://books.google.at/books?id=mqWK%5C_jXur-4C.

[13] J.C. Gascard. “Vertical motions in a region of deep water formation”. In: *Deep Sea Research and Oceanographic Abstracts* 20.11 (1973), pp. 1011–1027. URL: https://www.sciencedirect.com/science/article/pii/0011747173900727.

[14] B. Grisogono. “A generalized Ekman layer profile with gradually varying eddy diffusities”. In: *Quarterly Journal of the Royal Meteorological Society* 121 (1995), pp. 445–453.

[15] B. Grisogono. “The angle of the near-surface wind-turning in weakly stable boundary layers”. In: *Quarterly Journal of the Royal Meteorological Society* 137.656 (2011), pp. 700–708. eprint: https://rmets.onlinelibrary.wiley.com/doi/pdf/10.1002/qj.789. URL: https://rmets.onlinelibrary.wiley.com/doi/abs/10.1002/qj.789.

[16] J.R. Holton and G.J. Hakim. *An Introduction to Dynamic Meteorology*. International Geophysics. Elsevier Science, 2013. URL: https://books.google.at/books?id=-ePQ6x6VbjgC.

[17] R. Huntford. *Nansen: The Explorer as Hero*. Little, Brown Book Group, 2012. URL: https://books.google.at/books?id=uOvKCQInwUQC.

[18] R. Huntford. *Roland Huntford Nansen Biography Huntf*. Hodder & Stoughton, 1999. URL: https://books.google.at/books?id=4WX1HAAACAAJ.

[19] O. S. Madsen. “A Realistic Model of the Wind-Induced Ekman Boundary Layer”. In: *Journal of Physical Oceanography* 7 (1977), pp. 248–255.

[20] J. Marshall and R.A. Plumb. *Atmosphere, Ocean, and Climate Dynamics: An Introductory Text*. Academic Press. Elsevier Academic Press, 2008. URL: https://books.google.at/books?id=uKXrlAEACAAJ.

[21] J. Milnor. “Analytic Proofs of the "Hairy Ball Theorem" and the Brouwer Fixed Point Theorem”. In: *The American Mathematical Monthly* 85.7 (1978), pp. 521–524. URL: http://www.jstor.org/stable/2320860.

[22] F. Nansen. *Scientific Results: The Oceanography of the North Polar Basin*. Bd. 3;Bd. 9. Brøgger, 1902. URL: https://books.google.at/books?id=d6eXmAEACAAJ.

[23] O. Parmhed, I. Kos, and B. Grisogono. "An Improved Ekman Layer Approximation for Smooth eddy Diffusivity Profiles". In: *Boundary-Layer Meteorology* 115.3 (2005), pp. 399–407.

[24] G.L. Pickard, L.D. Talley, and W.J. Emery. *Descriptive Physical Oceanography*. Elsevier Science, 1990. URL: https://books.google.at/books?id=94GNMv57uH8C.

[25] R. H. Rapp. "Current estimates of mean Earth ellipsoid parameters". In: *Geophysical Research Letters* 1.1 (1974), pp. 35–38. eprint: https://agupubs.onlinelibrary.wiley.com/doi/pdf/10.1029/GL001i001p00035. URL: https://agupubs.onlinelibrary.wiley.com/doi/abs/10.1029/GL001i001p00035.

[26] J. Röhrs and K.H. Christensen. "Drift in the uppermost part of the ocean". In: *Geophysical Research Letters* 42.23 (2015), pp. 10, 349–10, 356. eprint: https://agupubs.onlinelibrary.wiley.com/doi/pdf/10.1002/2015GL066733. URL: https://agupubs.onlinelibrary.wiley.com/doi/abs/10.1002/2015GL066733.

[27] O. Stepanyuk et al. "Factors affecting atmospheric vertical motions as analyzed with a generalized omega equation and the OpenIFS model". In: *Tellus A: Dynamic Meteorology and Oceanography* 69.1 (2017), p. 1271563. eprint: https://doi.org/10.1080/16000870.2016.1271563. URL: https://doi.org/10.1080/16000870.2016.1271563.

[28] Z.-M. Tan. "An Approximate Analytical Solution For The Baroclinic And Variable eddy Diffusivity Semi-Geostrophic Ekman Boundary Layer". In: *Boundary-Layer Meteorology* 98.3 (2001), pp. 361–385.

[29] G. Teschl. *Ordinary Differential Equations and Dynamical Systems*. Graduate studies in mathematics. American Mathematical Society, 2012. URL: https://books.google.at/books?id=FZ0CAQAAQBAJ.

[30] S. Waggy, S. Marlatt, and S. Biringen. "Direct Simulation of the Turbulent Ekman Layer: Evaluation of Closure Models". In: *Journal of the Atmospheric Sciences* 69 (2009).

[31] Y. Yoshikawa and A. Masuda. "Seasonal variations in the speed factor and deflection angle of the wind-driven surface flow in the Tsushima Strait". In: *Journal of Geophysical Research: Oceans* 114.C12 (2009). eprint: https://agupubs.

onlinelibrary.wiley.com/doi/pdf/10.1029/2009JC005632. URL: https://agupubs.onlinelibrary.wiley.com/doi/abs/10.1029/2009JC005632.